Journal of Power Sources, 43–44 (1993) 603–610

Reversible potassium vanadium bronze cathodes ($K_xV_6O_{13+y}$) with various potassium to vanadium ratios

E. Andrukaitis

Directorate Research and Development, Air Research and Development Branch, 101 Colonel By Drive, Ottawa, Ont., K1A 0K2 (Canada)

Abstract

Electrodes composed of crystalline $K_xV_6O_{13+y}$, where $0.0 \leqslant x \leqslant 3.7$ and $0.1 \leqslant y \leqslant 3.1$, were prepared by thermal decomposition of electrochemically-deposited $(NH_4)_xK_{4-x}V_6O_{16}$ phases at 300 to 350 °C. The reversible lithium insertion into these materials was measured under cyclic voltammetry and constant current conditions. Phase changes during discharge resembled those of V_2O_5 or V_6O_{13} for similar vanadium oxidation states and small K/V ratios ($\leqslant 0.3$). The reversible capacity decreased as the K/V ratios increased from 0.1 to 0.5 and was small above K/V = 0.5 (Li/V < 0.1). The reversible capacity of the bronzes improved for lower O/V ratios, but best cycle life was obtained for nonstoichiometric vanadium oxides with K/V ratios in the range of 0.05 to 0.3 for O/V ratios between 2.0 to 2.5. Over 50 cycles at the *C*-rate were obtained with 5 to 10% of the capacity lost at 0.4 e^-/vanadium depth-of-discharge.

Introduction

Most of the work on vanadium oxides as secondary cathodes has focused on V_2O_5, V_6O_{13} and LiV_3O_8 and to a lesser extent on heteroatom vanadium bronzes [1]. The vanadium pentoxide bronze phases, $M_xV_2O_5$, where M = Li, Na, K, Mg, Ca or Ag, have been known for a long time [2] and the intercalation ability of some of these phases was studied [3–5]. The bronzes with M = Na, K, Cs and Ca were found to form by the electrochemical reduction of V_2O_5 in molten dimethylsulfone electrolytes and the reversible intercalation was dependent on the guest cationic species [5]. Ryan [6] found that $K_3V_5O_{14}$ gave better performance than V_2O_5 as high-energy cathodes for thermal cells. Pouchard *et al.* [7] plotted a composition diagram of the ranges of existence of homogeneous solid phases in the V_2O_5–V_2O_4–K_2O ternary system. This was extended to a quaternary system to include $(NH_4)_2O$ [8]. It was found that the hexavanadate lattices were sufficiently open to permit rather limited replacement of one of the ions K^+, Rb^+, Cs^+ or NH_4^+ with Li^+, but at a slow rate and small capacity [8].

This paper studies bronzes obtained by the thermal decomposition of electrochemically-prepared $(NH_4)_xK_{4-x}V_6O_{16+y}$, where $0.0 \leqslant x \leqslant 4.0$ and $0.0 \leqslant y \leqslant 0.1$. The electrochemical insertion of Li^+ in these $K_xV_6O_{13+y}$ bronzes, with various K/V and O/V ratios, will be discussed.

Experimental

The conducting supports (nickel sheet (0.2 mm), platinum (0.2 mm), nickel mesh (0.05 mm) and copper mesh (0.3 mm)) were cleaned and other materials were purified,

0378-7753/93/$6.00

as described previously [8, 9]. Deposition solutions were prepared by adding a standard 0.5 M KVO_3 to a NH_4VO_3 solution at 50 °C ($\approx$0.5 M), to a total cell volume of 250 cm^3. The electrodeposits were formed on conducting substrates by cyclic voltammetry from +0.2 to −0.7 V at 50 mV/s for several hours. The deposits were rinsed in distilled water, dried and then thermally decomposed from 300 to 350 °C in a tube furnace under air, vacuum (1 mm Hg) or inert gas (argon) atmospheres. Electrodeposits were analyzed by scanning electron microscopy (SEM), X-ray powder diffraction (XRD), inductively coupled plasma spectroscopy (ICP), and chemical analysis [8].

Electrochemical experiments were performed in an argon-filled glove box at ambient temperature. The cell consisted of a counter, working, and reference electrodes of lithium metal, vanadium oxide bronze and Ag/AgCl respectively. The electrolyte was 0.5 M lithium perchlorate in propylene carbonate (PC). Cyclic voltammetry and constant currents were applied using a PAR Model 273 potentiostat. The amount of lithium intercalated was determined by analysis and compared with the total charge passed.

Results and discussion

Formation of electrodes

The details of the formation and nature of the electrodeposits $M_xM'_{4-x}V_6O_{16+y}$, with M, M' = K, Rb, Cs or NH_4, $0.0 \leqslant x \leqslant 4.0$ and $0.00 \leqslant y \leqslant 0.13$ as well as the heating of $(NH_4)_4V_6O_{16}$ in air to form V_2O_5 have been discussed previously [8, 9]. A more systematic formation of mixed phases with a given K/V ratio was done by varying the amount of a standard KVO_3 solution in saturated NH_4VO_3 at 50 °C. By the use of cyclic voltammetry, deposits with a range of K/V from 0.0 to 0.63 were formed on conducting substrates with similar orientation and structure to electrodeposited $(NH_4)_4V_6O_{16}$ and $K_4V_6O_{16}$ [9]. The $(NH_4)_{4-x}K_xV_6O_{16}$ deposits were homogeneous and crystalline with a progression from one single phase to the other as the NH_4^+ was replaced by K^+, with only minor shifts in their diffraction angles [8].

The thermal decomposition of the $(NH_4)_{4-x}K_xV_6O_{16}$ electrodeposits gave bronzes with a $K_xV_6O_{13+y}$ stoichiometry. The X-ray diffraction patterns of various bronzes are shown in Fig. 1. For small K/V ratios (<0.1) the X-ray pattern was similar to V_2O_5 (heated in air) and V_6O_{13} (in vacuum) and for large K/V values (>0.55) to $K_4V_6O_{16}$ [9]. Intermediate K/V ratios had major peaks which matched no known potassium vanadium oxide (or K_xO) single phase. They appeared to be associated with the addition of K which shifted the diffraction angles of certain lines, increasing the d-spacing, from the one parent oxide (V_2O_5 or V_6O_{13}) to the other ($K_4V_6O_{16}$) [8]. Details of the structural changes and the decomposition of the bronzes will be discussed elsewhere.

The location of these phases on the composition diagram with the ranges of existence of homogeneous solid phases in the V_2O_5–V_2O_4–K_2O–$(NH_4)_2O$ quaternary system [8] have been plotted in Fig. 2. Except for the $(NH_4)_xK_{4-x}V_6O_{16}$ electrodeposits (cross hatched), which lie on a narrow surface bounded by the line bb' (on the plane $(NH_4)_2O$–c–K_2O) and a corresponding line on the plane $(NH_4)_2O$–c'–K_2O), all other data in Fig. 2 lie on the two front faces of the tetrahedron. The bronzes formed were expected to lie in an area bounded by the j($K_4V_6O_{17}$), j'($K_4V_6O_{15}$), d(V_6O_{13}) and V_2O_5. The actual bronzes made are given by open circles in Fig. 2. The air-heated bronzes, which undergo oxidation of V(IV) to V(V) during thermal decomposition, lie below the b'($K_4V_6O_{16}$)–c(V_3O_7) line. Vacuum-heating results in partial reduction of V(V) to V(IV) in the bronze so that they lie near or above the b'–c line.

Using thermal gravimetric (TGA) and chemical analysis, heating the deposit gave a mass loss which corresponded to the removal of NH_3 and H_2O with an overlapping

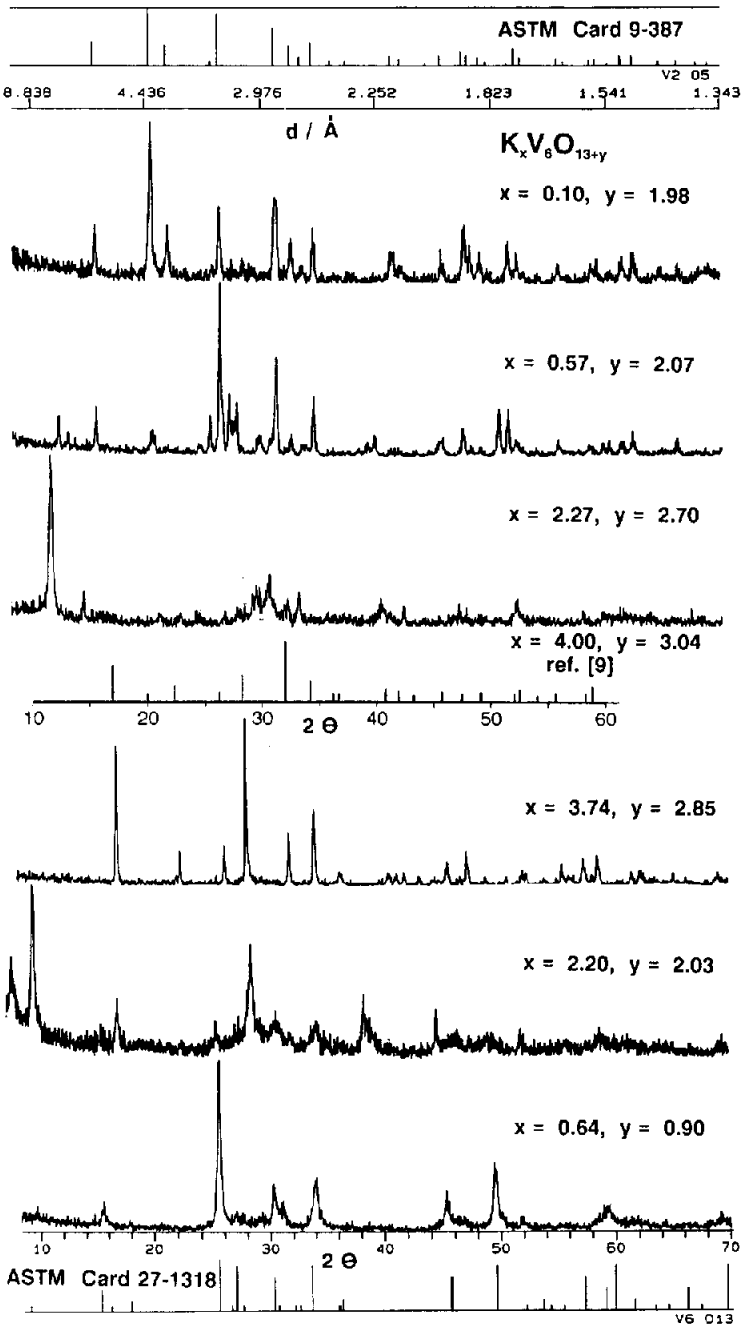

Fig. 1. X-ray diffraction spectrum of $K_xV_6O_{13+y}$ phases on a nickel substrate for x, y values: 0.10, 1.98; 0.57, 2.07; 2.27, 2.70; 3.74, 2.85; 2.20, 2.03, and 0.64, 0.90. Also shown are the ASTM X-ray stick patterns for V_2O_5, V_6O_{13} and $K_4V_6O_{16}$ ($x=4.00$, $y=3.04$) [9, 10]. All intensities are relative to the most intense line in each pattern.

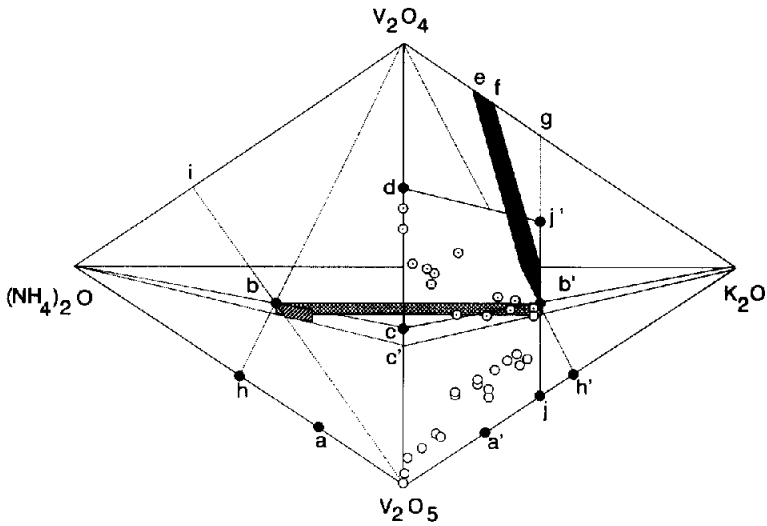

Fig. 2. Compositions of homogeneous phases in the quaternary system V_2O_5–V_2O_4–K_2O–$(NH_4)_2O$: (a, a') $(NH_4)_2V_6O_{16}$, $K_2V_6O_{16}$; (b, b') $(NH_4)_4V_6O_{16}$, $K_4V_6O_{16}$ [11]; (c, c') V_3O_7, $V_3O_{7.07}$; (d) V_6O_{13}; (e, f, g) $K_2V_8O_{17}$, $K_2V_6O_{13}$, $K_2V_3O_7$ [7]; (h, h') NH_4VO_3, KVO_3; (i) $(NH_4)_2V_3O_7$; (j, j') $K_4V_6O_{17}$, $K_4V_6O_{15}$. Solid area: results of [11]; horizontal hatching: results of [7]; cross hatching: results of [8]; open circles: phases studied for lithium intercalation in this paper formed by thermal decomposition of $(NH_4)_xK_{4-x}V_6O_{16}$ at 350 °C in air; with centre dot, under vacuum.

mass gain or loss (oxidation of the bronze in air or reduction in inert atmosphere, respectively) forming the $K_xV_6O_{13+\delta}$ bronze. The air decomposition was found to involve similar reaction steps to the heating of $(NH_4)_4V_6O_{16}$ deposits [9]. The overall reaction in air was:

$$(NH_4)_xK_{4-x}V_6O_{16}+y/2O_2 \longrightarrow K_{4-x}V_6O_{16+y-x/2}+xNH_3+x/2H_2O \quad (1)$$

The final oxidation step: $V_2O_{5-y}+y/2O_2 \rightarrow V_2O_5$, seen for $(NH_4)_4V_6O_{16}$, was influenced by the presence of K and the oxidation of V(IV) to V(V) was incomplete. The air-decomposed bronzes lie in a narrow V(IV)/(total K–V(IV)–V(V)) band of 10 to 15% for K/V from 0.1 to 0.6 (Fig. 2). The oxidation step was influenced by the decomposition temperature and time as well as the presence of K.

Decomposition of $(NH_4)_4V_6O_{16}$ to form V_6O_{13} has been observed by other researchers [11]. The presence of K^+ also influenced the reduction of V(V) to V(IV). The decomposition of the deposit under an oxygen deficient atmosphere (argon or vacuum) resulted in the formation of bronzes by the overall reaction:

$$(NH_4)_xK_{4-x}V_6O_{16} \longrightarrow K_{4-x}V_6O_{16-y-x/2}+xNH_3+x/2H_2O+y/2O_2 \quad (2)$$

where reduction of some of the V(V) to V(IV) occurred. The bronzes had a broader band of stoichiometry with a V(V)/(total K–V(IV)–V(V)) range of about 40 to 50% for K/V from 0.1 to 0.6 (Fig. 2).

Electrochemical insertion into electrodes

The phase changes occurring during discharge depended on the $K_xV_6O_{13+y}$ stoichiometry. The initial discharge curves for air-decomposed bronzes with different K/V ratios are shown in Fig. 3(a). The phase changes were similar and occurred at

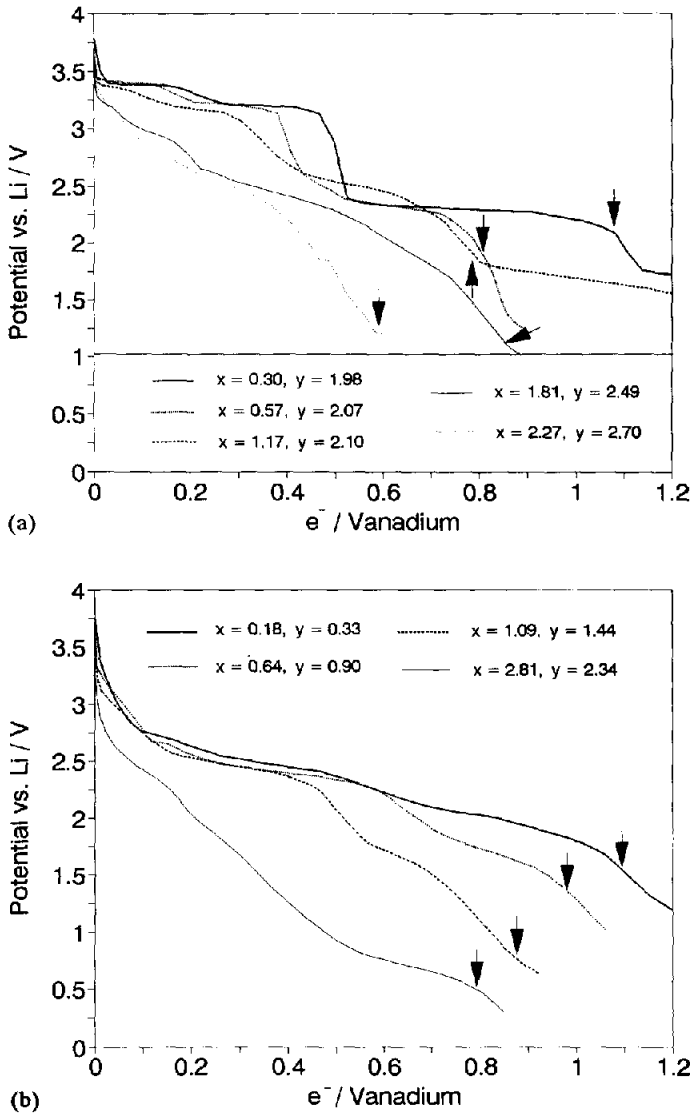

Fig. 3. (a) Initial discharge curves of $K_xV_6O_{13+y}$ in 1 M $LiClO_4$/PC at a current density of 0.5 mA/cm^2. Phases produced by thermal decomposition of ammonium containing electrodeposits in air with the x, y values: 0.30, 1.98; 0.57, 2.07; 1.17, 2.10; 1.81, 2.49; and 2.27, 2.70. Arrows near end of discharge indicate the amount of lithium inserted from chemical analysis. (b) Initial discharge curves of $K_xV_6O_{13+y}$ phases produced by thermal decomposition of electrodeposits in vacuum with the x, y values: 0.18, 0.33; 0.64, 0.90; 1.09, 1.44; and 2.81, 2.34.

the same depth-of-discharge (e^-/vanadium) as those of V_2O_5 when the $K/V \leqslant 0.05$ [9]. For $K/V \geqslant 0.1$, the initial flat voltage plateau at about 3.3 V (versus lithium) was shorter and the second plateau occurred at $e^-/V = 0.4$ to 0.45. In this region of the

discharge the V_2O_5 bronze disproportionates [2, 12] and the reversibility was diminished. The lithium intercalation was impeded at higher K/V ratios because of the steric interference of the K^+ between the vanadium oxide layers. The initial capacity for Li^+ to the large potential drop (δ bronze phase [13]) decreased in proportion to the increase in K^+ present. For $K/V \geq 0.3$, the phase changes were no longer distinct and the Li insertion capacity dropped to about 0.1 e^-/V at $K/V = 0.5$ (Table 1(a)). The reversible insertion of Li was best when the depth-of-discharge was limited to 0.5 e^-/V (prior to δ bronze phase) but very low capacity discharges had to be used for large K/V ratios.

Initial discharge curves for the vacuum decomposed bronzes are shown in Fig. 3(b). The discharge curves were similar to those of nonstoichiometric V_6O_{13} [14] for $K/V < 0.05$ and the capacity for insertion again decreased for larger K/V ratios to a 1.5 V cutoff voltage (Table 1(b)). The lower O/V ratio phases (higher V(IV)/V ratio) exhibited a greater reversible capacity for similar K/V ratios. These bronze structures may be more suitable than higher O/V phase for secondary cathodes with their larger depth-of-discharge, but the number of cycles increased as the K/V ratio increased.

The lower cycle life of vacuum prepared bronzes at low K/V ratios are due to the use of a higher depth-of-discharge, the poor adherence of these bronzes to the conducting substrate and a capacity increase over the first several cycles for bronzes

TABLE 1.

(a) Summary of chemical and inductively coupled plasma spectroscopy (ICP) analysis of potassium bronzes by decomposition of $(NH_4)_xK_{4-x}V_6O_{16}$ in air and electrochemically-discharged and cycled (to a 2.0 V cutoff)

KVO_3, in solution (ml)[a]	ICP K/V	Chemical analysis V(IV)/V(tot)	$K_xV_6O_{13+y}$[b]		Maximum Li inserted (e^-/V)	No. cycles and final capacity[c]
			(x)	(y)		
2	0.016	0.025	0.10	1.98	1.08	30 (0.97)
5	0.050	0.056	0.30	1.98	1.05	45 (0.94)
15	0.095	0.072	0.57	2.07	0.86	31 (0.89)
60	0.195	0.161	1.17	2.10	0.80	20 (0.90)
100	0.302	0.140	1.81	2.49	0.84	20 (0.67)
120	0.378	0.145	2.27	2.70	0.69	25 (0.79)
150	0.508	0.151	3.05	3.07	0.10	25 (0.76)

(b) Summary of chemical and ICP analysis of potassium bronzes by heating of $(NH_4)_xK_{4-x}V_6O_{16}$ in vacuum and electrochemically-discharged and cycled (to a 1.5 V cutoff)

0	0.000	0.618	0.00	0.15	1.12	10 (0.92)
2	0.030	0.587	0.18	0.33	1.09	22 (0.78)
15	0.106	0.474	0.65	0.90	0.94	10 (0.95)
60	0.182	0.368	1.09	1.44	0.83	22 (0.93)
120	0.367	0.357	2.20	2.03	0.52	40 (0.88)
150	0.468	0.355	2.81	2.34	0.79	38 (0.81)

[a]Value given are volume of standard 0.5 M KVO_3 added to saturated aqueous NH_4VO_3 to total volume of 250 cm^3.

[b]Calculation of bronze stoichiometry assumes charge balance, see ref. 8 for details.

[c]Is the fraction of initial capacity on final discharge before analysis (at a C-rate discharge).

with a high K/V ratio. The best results were obtained when fine nickel mesh substrates were used, but more improvement in the adherence of these particular bronzes was needed. In the past, the tetrametal hexavanadate lattices have been found to be sufficiently open to permit rather limited replacement of one of the ions K^+, Rb^+, Cs^+ or NH_4^+ with Li^+, but at a slow rate, unless the lattice was subjected to severe cyclic oxidation and reduction [8]. The replacement of K^+ with Li^+ was also found to occur in the $K_xV_6O_{13+y}$ bronzes. A capacity gain over the first 10 to 20 cycles (sometimes up to 100% at K/V = 0.30) was observed as some of the K^+ was removed from the bronze on charge and replaced with Li^+ on discharge under normal discharge and charge cycling (*C*-rate from 4.5 to 1.5 V). The higher solubility of bronzes with large amounts of V(IV) (at the lower K/V ratios) and the movement of K^+ during cycling will be examined in more detail.

Conclusion

The thermal decomposition of $(NH_4)_xK_{4-x}V_6O_{16}$ proceeded via different mechanisms under air or inert atmospheres and by the loss of NH_3 and H_2O resulted in the formation of adherent, oriented, crystalline $K_xV_6O_{13+y}$ electrodes, where $0.0 \leqslant x \leqslant 3.7$ and $0.1 \leqslant y \leqslant 3.1$. The value of y depended on the amount of K and the V(IV)/V(V) ratio in the bronze. The oxidation of all the V(IV) or partial reduction of V(V) depended on the amount of K^+ present as well as the decomposition temperature. Nonstoichiometric oxides similar in structure to V_2O_5 or V_6O_{13} for small K/V ratios and $K_4V_6O_{16}$ for large K/V values were obtained. Electrodes formed by decomposition in air with a nonstoichiometric V_2O_5 structure (K/V from 0.05 to 0.1, O/V from 2.4 to 2.5) gave the best cycle life with operating voltages above 2.5 V. Over 50 cycles were obtained with a 5 to 10% capacity loss at a 0.4 e^-/V depth-of-discharge (*C*-rate).

These electroformed bronzes show structures and properties unique to those prepared by high-temperature synthesis. A close relation exists to their parent oxides, with the bronze structure and lithium insertion influenced by the presence of K^+.

Acknowledgements

J. Smit of the Electrochemical Science and Technology Centre Ottawa is thanked for technical assistance and J. Loop from the Ottawa Carleton Geoscience Centre is thanked for ICP analysis.

References

1 J. Desilvestro and O. Haas, *J. Electrochem. Soc., 137* (1990) 5C–22C.
2 P. Hagenmuller, in J. C. Bailar, H. J. Emeleus, R. Nyholm and A. F. Trotman-Dickenson (eds.), *Comprehensive Inorganic Chemistry,* Vol. 4, Pergamon, Oxford, 1973, pp. 569–601.
3 I. Raistrick and R. Huggins, *Mater. Res. Bull., 18* (1983) 337.
4 I. Raistrick, *Rev. Chim. Miner., 21* (1984) 456.
5 J. P. Pereira-Ramos, R. Messina and J. Perichon, *J. Electrochem. Soc., 135* (1988) 3050–3057.
6 D. M. Ryan, *Proc. 25th Intersociety Energy Conversion Engineering Conf., Reno, NV, USA, Aug. 12–17, 1990,* pp. 110–113.

7 M. Pouchard, J. Galy, L. Rabardel and P. Hagenmuller, *CR Acad. Sci., 264* (1967) 1943–1946.
8 E. Andrukaitis, J. W. Lorimer and P. W. M. Jacobs, *Can. J. Chem., 68* (1990) 1283–1292.
9 E. Andrukaitis, P. W. M. Jacobs and J. W. Lorimer, *Solid State Ionics, 37* (1990) 157–169.
10 *ASTM,* Philadelphia, PA, 1962, Cards 9–387 and 27–1318.
11 J. Bernard, F. Theobald and A. Vidonne, *Bull. Soc. Chim. Fr., 6* (1970) 2108.
12 B. Liaw, I. D. Raistick and R. A. Huggins, Solid State Ionics, 18/19 (1986) 828–832.
13 M. S. Whittingham, *J. Electrochem. Soc., 123* (1976) 315.
14 K. M. Abraham, J. L. Goldman and M. D. Dempsey, *J. Electrochem. Soc., 128* (1981) 2493–2501.